Histopathological changes

NFT treatment induced hyaline droplet degeneration of proximal tubules in the cortex from day 3 of treatment, and scattered proximal tubular regeneration in the cortex and OSOM at day 28. Similar to a previous report (NTP, 1996), ADAQ treatment induced hyaline droplet degeneration of proximal tubules in the cortex from day 3 of treatment, and proximal tubular pigmentation in the OSOM and scattered tubular regeneration in the cortex and OSOM at day 28. TCP treatment induced proximal tubular cell karyomegaly accompanied with diffuse regenerative hyperplasia in the OSOM from day 3, similar to previous report (NTP, 1993a). CP treatment induced marginal hyaline droplet degeneration of proximal tubules in the cortex at day 28. TAT treatment induced hyaline droplet degeneration of proximal tubules in the cortex, and scattered tubular regeneration in the cortex and OSOM at day 28, similar to previous report (NTP, 1993b). CBX treatment induced scattered tubular regeneration in the cortex and OSOM, and hyaline cast in the Henle's thin segment and collecting tubules, accompanied with diffuse regeneration of collecting tubules at day 28.

Distribution of immunoreactive cells and apoptotic cells

Ki-67, p-Histone H3, TOP2A, and p-MDM2 were immunolocalized in the nucleus of tubular epithelial cells, and UBD was immunolocalized in the cytoplasm or mitotic spindle of tubular epithelial cells (Figs. 1-3). TUNEL$^+$ apoptotic cells were also observed in tubular epithelial cells (Figs. 1-3). Ki-67$^+$, p-Histone H3$^+$, TOP2A$^+$, UBD$^+$, and TUNEL$^+$ cells were evenly distributed in the renal tubules within the kidney. With regard to p-MDM2, immunoreactive cells were predominantly observed in distal tubular epithelial cells.

At day 3, the number of Ki-67$^+$ cells significantly increased in the NFT, TCP, and CBX groups, and significantly decreased in the ADAQ and TAT groups compared with untreated controls (Fig. 1A). The number of p-Histone H3$^+$ cells significantly increased in the NFT and TCP groups, and significantly decreased in the TAT group compared with untreated controls (Fig. 1B). The number of TOP2A$^+$ cells significantly increased in the NFT, TCP, CP, and CBX groups, and significantly decreased in the ADAQ and TAT groups compared with untreated controls (Fig. 1C). The number of UBD$^+$ cells significantly increased in the NFT, TCP, and CBX groups, and significantly decreased in the ADAQ and TAT groups compared with untreated controls (Fig. 1D). The number of p-MDM2$^+$ cells significantly decreased in the NFT, ADAQ, TCP, CP, and TAT groups compared with untreated controls (Fig. 1E). The number of TUNEL$^+$ cells did not change in any of the treatment groups (Fig. 1F).

At day 7, the number of Ki-67$^+$ cells significantly increased in the NFT and TCP groups, and significantly decreased in the ADAQ and TAT groups compared with untreated controls (Fig. 2A). The number of p-Histone H3$^+$ cells significantly increased in the NFT group, and significantly decreased in the CP group compared with untreated controls (Fig. 2B). The number of TOP2A$^+$ cells significantly increased in the TCP group, and significantly decreased in the ADAQ and TAT groups compared with untreated controls (Fig. 2C). The number of UBD$^+$ cells significantly increased in the TCP group, and significantly decreased in the ADAQ and TAT groups compared with untreated controls (Fig. 2D). The number of p-MDM2$^+$ cells did not change in any of the treatment groups (Fig. 2E). The number of TUNEL$^+$ cells significantly increased in the NFT and TCP groups compared with untreated controls (Fig. 2F).

At day 28, the number of Ki-67$^+$ cells significantly increased in the NFT, ADAQ, TCP, and CBX groups compared with untreated controls (Fig. 3A). The number of p-Histone H3$^+$ cells significantly increased in the NFT and CBX groups compared with untreated controls (Fig. 3B). The number of TOP2A$^+$ cells significantly increased in the ADAQ, TCP, and CBX groups compared with untreated controls (Fig. 3C). The number of UBD$^+$ cells significantly increased in the ADAQ, TCP, and CBX groups compared with untreated controls (Fig. 3D). The number of p-MDM2$^+$ cells significantly increased in the TCP group, and significantly decreased in the NFT and CP groups compared with untreated controls (Fig. 3E). The number of TUNEL$^+$ cells significantly increased in the CBX group compared with untreated controls (Fig. 3F).

p-Histone H3$^+$/Ki-67$^+$ cell ratio

To estimate the number of proliferative cells existing at M phase, the ratio of the number of p-Histone H3$^+$ cells to that of Ki-67$^+$ cells was calculated using data obtained from kidney slides immunohistochemically stained for each molecule in the same animal.

At day 3, the ratio of the number of p-Histone H3$^+$ cells to that of Ki-67$^+$ cells significantly decreased in the TCP group compared with the untreated controls (Fig. 4A). At day 7, the ratio of the number of p-Histone H3$^+$ cells to that of Ki-67$^+$ cells significantly decreased in the TCP group compared with untreated controls (Fig. 4B). At day 28, the ratio of the number of p-Histone H3$^+$ cells to that of Ki-67$^+$ cells significantly decreased in the ADAQ and TCP groups compared with the untreated controls (Fig. 4C).

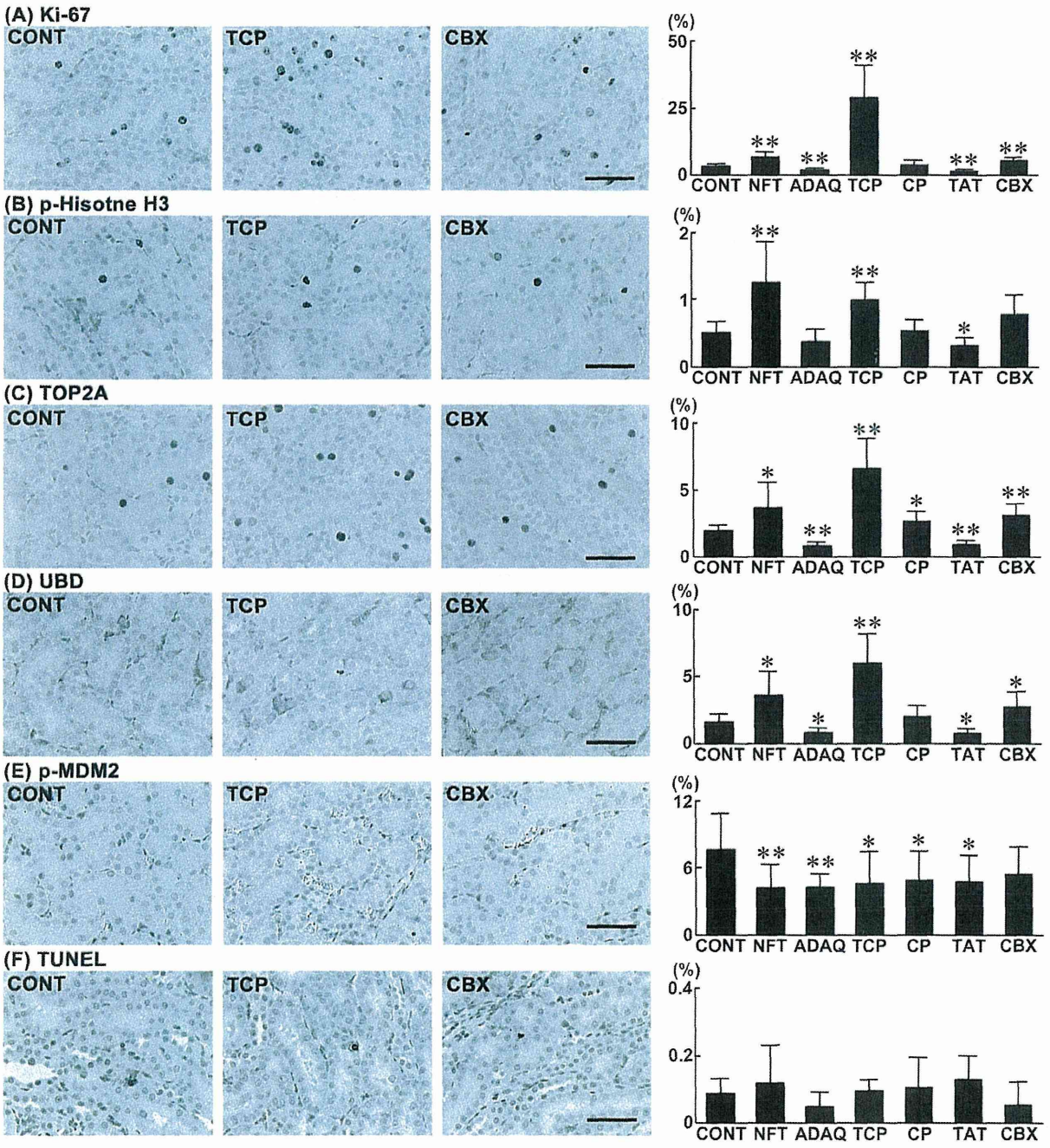

Fig. 1. Distribution of Ki-67$^+$, p-Histone H3$^+$, TOP2A$^+$, UBD$^+$, p-MDM2$^+$, and TUNEL$^+$ cells in the OSOM of rats at day 3 after treatment with renal carcinogens or non-carcinogenic renal toxicants. Photomicrographs show the distribution of Ki-67$^+$, p-Histone H3$^+$, TOP2A$^+$, UBD$^+$, p-MDM2$^+$, and TUNEL$^+$ cells in the OSOM of representative cases from untreated controls and animals treated with TCP or CBX. The graphs show positive cell ratios of renal tubular epithelial cells per total cells counted in 10 animals of each group. Values represent mean + S.D. (A) Ki-67, (B) p-Histone H3, (C) TOP2A, (D) UBD, (E) p-MDM2, and (F) TUNEL. Bar = 50 μm. * $P < 0.05$, ** $P < 0.01$ vs. untreated controls (Dunnett's or Steel's test).

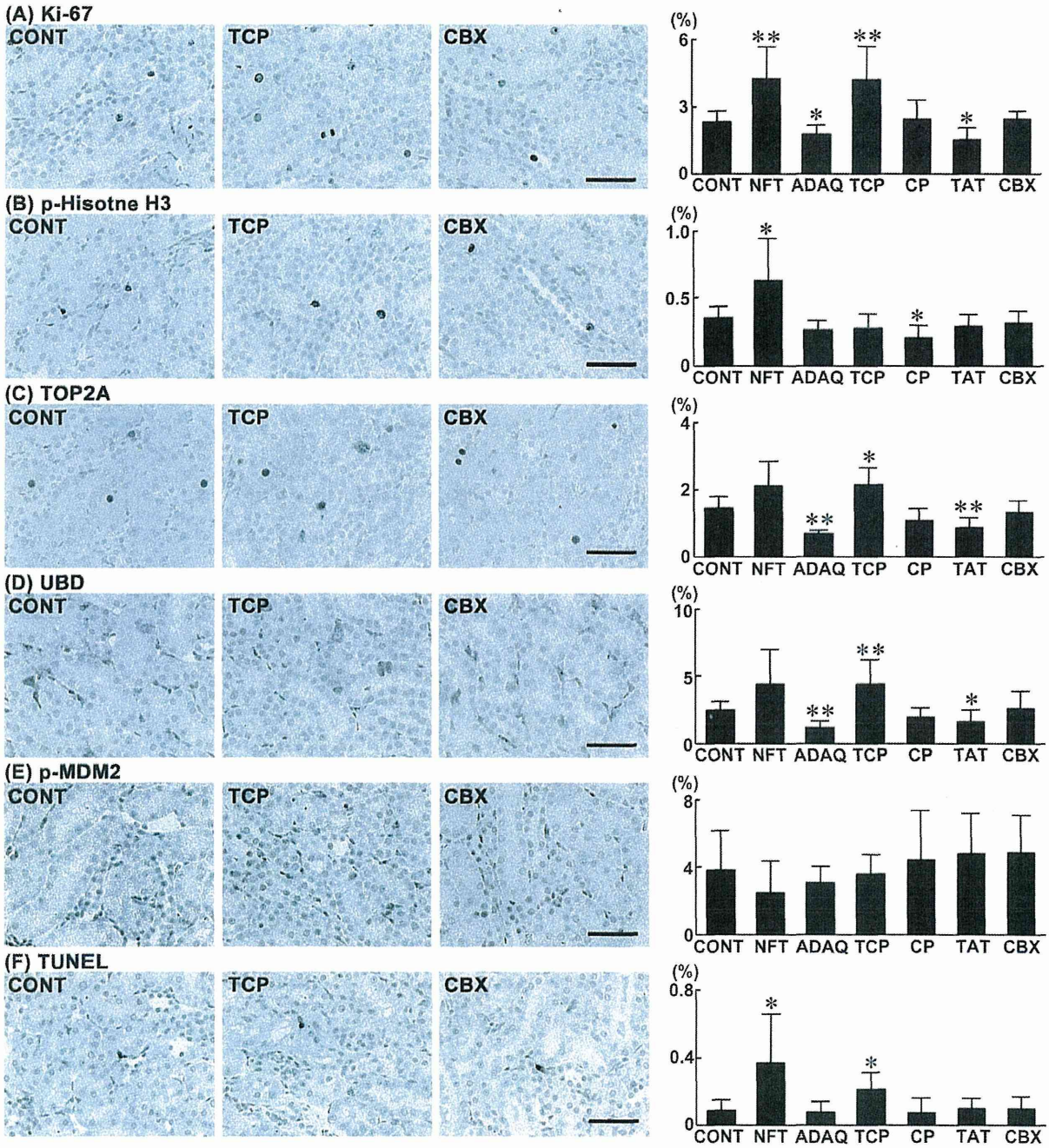

Fig. 2. Distribution of Ki-67$^+$, p-Histone H3$^+$, TOP2A$^+$, UBD$^+$, p-MDM2$^+$, and TUNEL$^+$ cells in the OSOM of rats at day 7 after treatment with renal carcinogens or non-carcinogenic renal toxicants. Photomicrographs show the distribution of Ki-67$^+$, p-Histone H3$^+$, TOP2A$^+$, UBD$^+$, p-MDM2$^+$, and TUNEL$^+$ cells in the OSOM of representative cases from untreated controls and animals treated with TCP or CBX. The graphs show positive cell ratios of renal tubular epithelial cells per total cells counted in 10 animals of each group. Values represent mean + S.D. (A) Ki-67, (B) p-Histone H3, (C) TOP2A, (D) UBD, (E) p-MDM2, and (F) TUNEL. Bar = 50 μm. * $P < 0.05$, ** $P < 0.01$ vs. untreated controls (Steel's test).

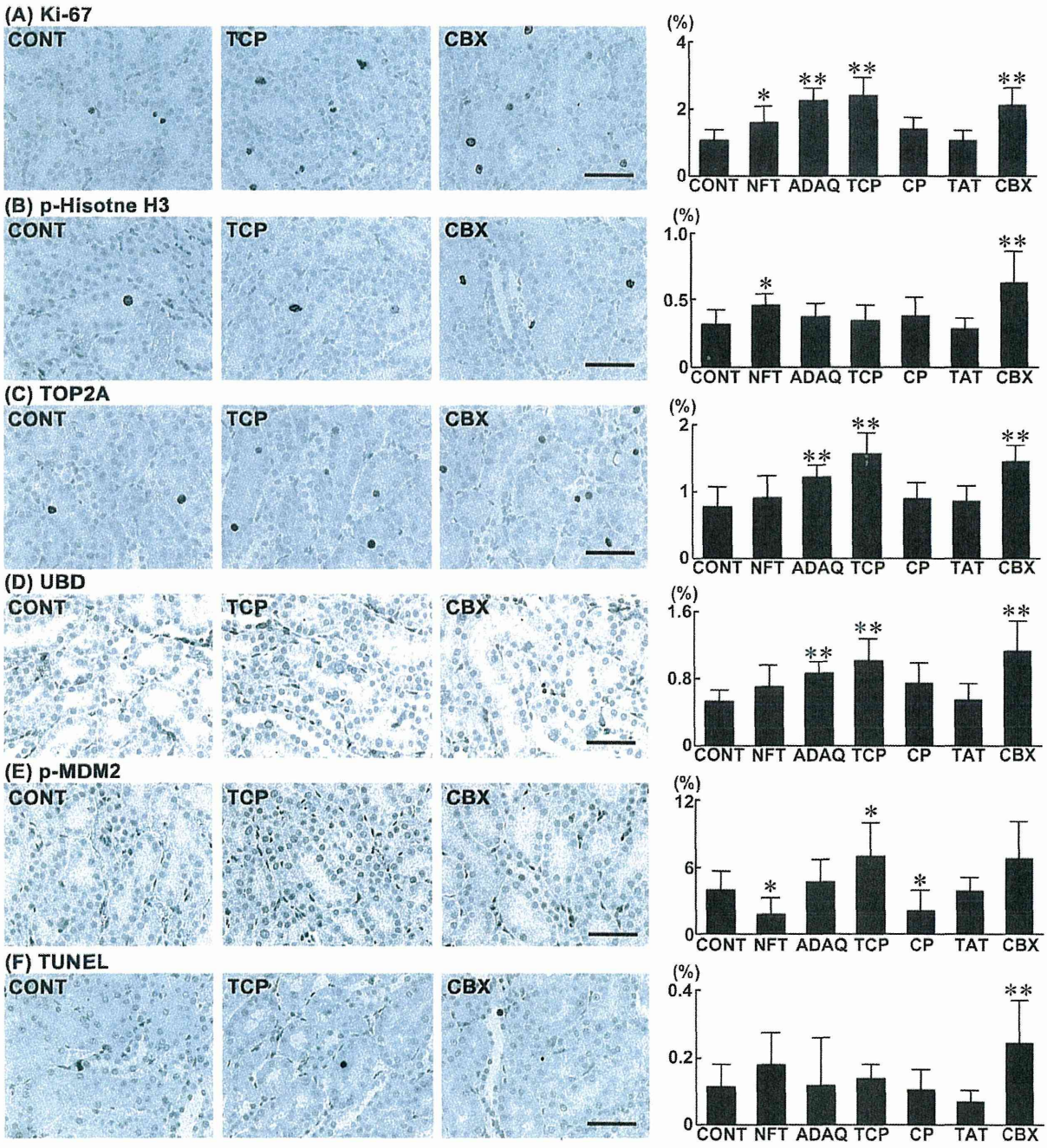

Fig. 3. Distribution of Ki-67$^+$, p-Histone H3$^+$, TOP2A$^+$, UBD$^+$, p-MDM2$^+$, and TUNEL$^+$ cells in the OSOM of rats at day 28 after treatment with renal carcinogens or non-carcinogenic renal toxicants. Photomicrographs show the distribution of Ki-67$^+$, p-Histone H3$^+$, TOP2A$^+$, UBD$^+$, p-MDM2$^+$, and TUNEL$^+$ cells in the OSOM of representative cases from untreated controls and animals treated with TCP or CBX. The graphs show positive cell ratios of renal tubular epithelial cells per total cells counted in 10 animals of each group. Values represent mean + S.D. (A) Ki-67, (B) p-Histone H3, (C) TOP2A, (D) UBD, (E) p-MDM2, and (F) TUNEL. Bar = 50 μm. * $P < 0.05$, ** $P < 0.01$ vs. untreated controls (Dunnett's or Steel's test).

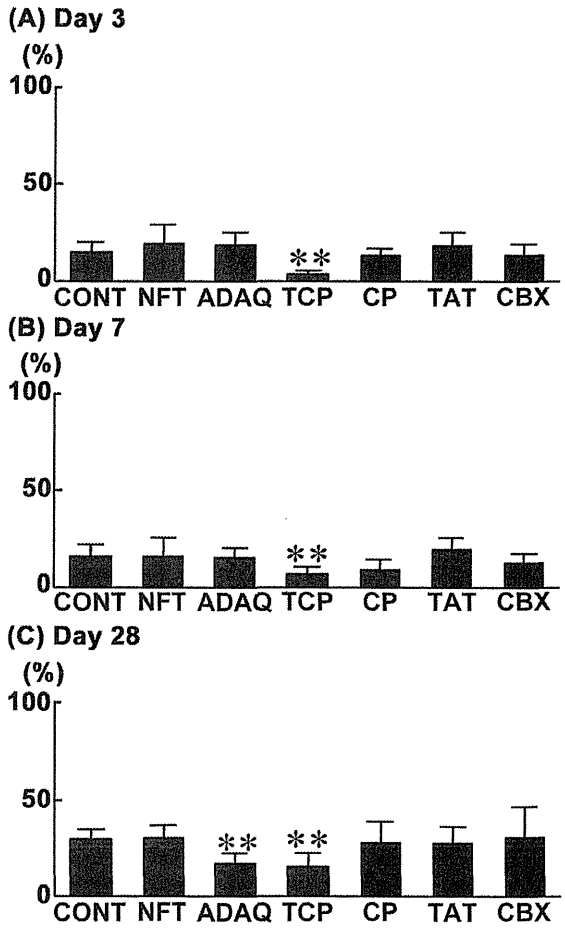

Fig. 4. p-Histone H3$^+$/Ki-67$^+$ cell ratio in the OSOM of rats at days 3, 7 and 28 after treatment with renal carcinogens or non-carcinogenic renal toxicants. The graphs show the p-Histone H3$^+$ cell ratio of renal tubular epithelial cells per number of Ki-67$^+$ cells counted in 10 animals of each group. Values represent mean + S.D. (A) Day 3, (B) Day 7 and (C) Day 28. ** $P < 0.01$ vs. untreated controls (Steel's test).

Colocalization of UBD with TOP2A or p-Histone H3

At day 3, the ratio of TOP2A$^+$ cells to the total number of UBD$^+$ cells did not change in any of the treatment groups (Fig. 5A). In contrast, the ratio of p-Histone H3$^+$ cells to the total number of UBD$^+$ cells significantly decreased in the TCP and CBX groups compared with the untreated controls (Fig. 5B).

At day 7, the ratio of TOP2A$^+$ cells to the total number of UBD$^+$ cells significantly increased in the TCP group compared with the untreated controls (Fig. 5C). The ratio of p-Histone H3$^+$ cells to the total number of UBD$^+$ cells significantly decreased in the TCP group compared with the untreated controls (Fig. 5D).

At day 28, the ratio of TOP2A$^+$ cells to the total number of the UBD$^+$ cells did not change in any of the treatment group (Fig. 5E). The ratio of p-Histone H3$^+$ cells to the total number of UBD$^+$ cells significantly decreased in the ADAQ and TCP groups compared with untreated controls (Fig. 5F).

Real-time RT-PCR analysis

Transcript levels of the genes listed in Supplementary Table 2 at days 3, 7 and 28 of treatment were determined by real-time RT-PCR in the NFT, ADAQ, TCP, and CBX groups, and compared with the levels in untreated controls (Supplementary Table 3).

At day 3, transcript levels of *Cdkn1a* (cyclin-dependent kinase inhibitor 1A) after normalization to *Actb* and/or *Gapdh* levels significantly increased in all treatment groups compared with untreated controls. Transcript levels of *Chek1* (checkpoint kinase 1) and *Mad2l1* (MAD2 mitotic arrest deficient-like 1 [yeast]) after normalization to *Actb* and/or *Gapdh* levels significantly increased in the NFT, TCP, and CBX groups, and significantly decreased in the ADAQ group compared with untreated controls. Transcript levels of *Mdm2* (MDM2 proto-oncogene, E3 ubiquitin protein ligase) after normalization to *Actb* and *Gapdh* levels significantly increased in the ADAQ, TCP, and CBX groups, and transcript levels of *Mdm2* after normalization to *Gapdh* levels significantly decreased in the NFT group compared with untreated controls. Transcript levels of *Rbl2* (retinoblastoma-like 2) after normalization to *Actb* levels significantly increased in the NFT and TCP groups compared with untreated controls. Transcript levels of *Tp53* (tumor protein p53) after normalization to *Actb* and/or *Gapdh* levels significantly increased in the TCP and CBX groups, and transcript levels of *Tp53* after normalization to *Gapdh* levels significantly decreased in the NFT group compared with untreated controls.

At day 7, transcript levels of *Cdkn1a*, *Chek1*, and *Mad2l1* after normalization to *Actb* and/or *Gapdh* levels significantly increased in the NFT and TCP groups compared with untreated controls. Transcript levels of *Cdkn1a* and *Mad2l1* after normalization to *Actb* and/or *Gapdh* levels significantly decreased in the ADAQ group compared with untreated controls. Transcript levels of *Mdm2* after normalization to *Actb* and/or *Gapdh* levels significantly increased in the ADAQ, TCP, and CBX groups compared with untreated controls. Transcript levels of *Tp53* after normalization to *Actb* and/or *Gapdh* levels significantly increased in all treatment groups compared with untreated controls. Transcript levels of *Rbl2* after normalization

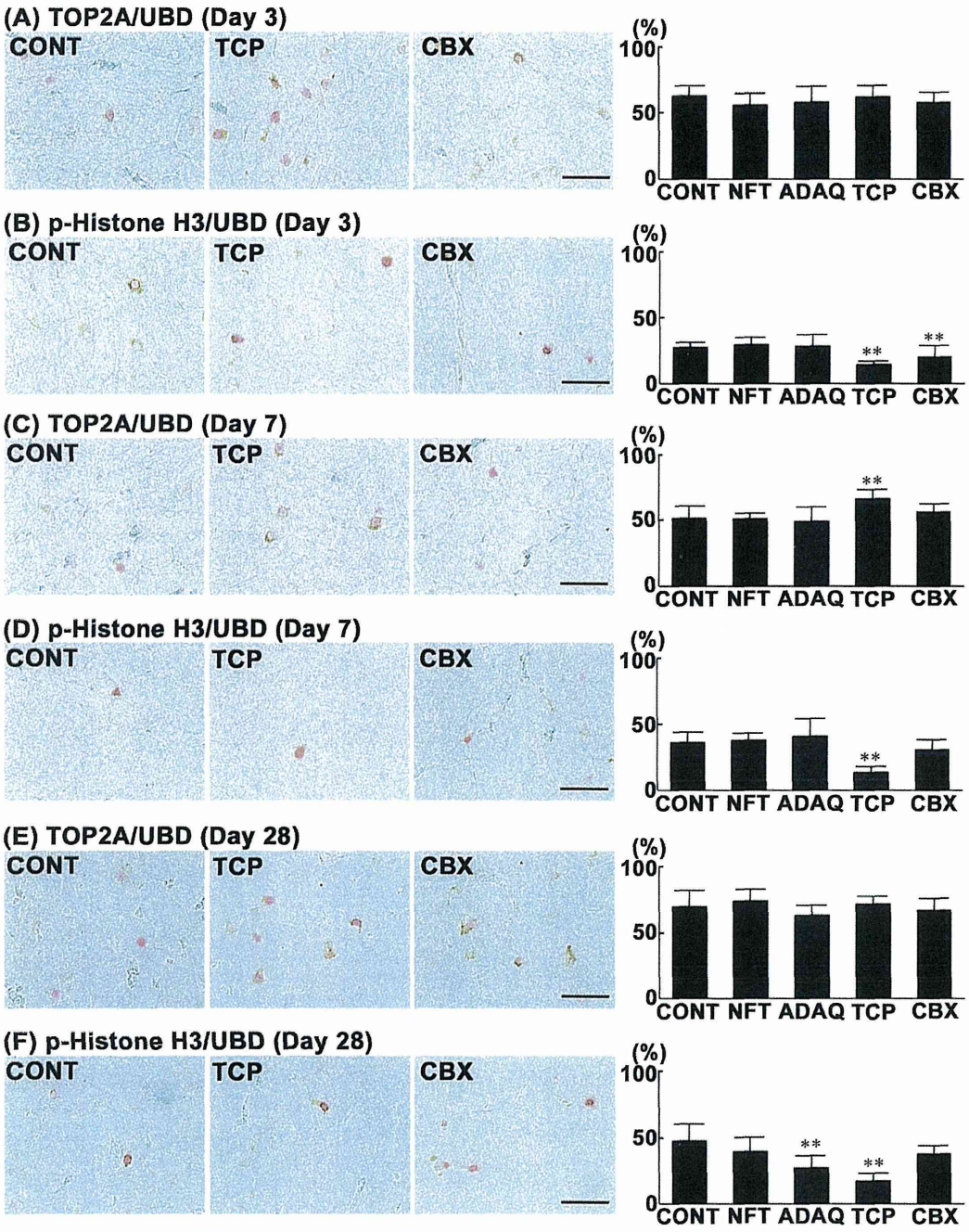

Fig. 5. Distribution of cell populations co-expressing UBD and TOP2A (TOP2A/UBD) or UBD and p-Histone H3 (p-Histone H3/UBD) in the OSOM of rats at days 3, 7 and 28. Photomicrographs show the distribution of TOP2A/UBD and p-Histone H3/UBD in the OSOM of representative cases from untreated controls and animals treated with TCP or CBX. The immunoreactivity of UBD (cytoplasm), and TOP2A (nucleus) or p-Histone H3 (nucleus) is visualized as brown and red, respectively. The graphs show the TOP2A or p-Histone H3-positive cell ratio (%) per total renal tubular epithelial cells immunoreactive to UBD counted in 10 animals of each group. Values represent mean + S.D. (A) TOP2A/UBD (day 3), (B) p-Histone H3/UBD (day 3), (C) TOP2A/UBD (day 7), (D) p-Histone H3/UBD (day 7), (E) TOP2A/UBD (day 28), and (F) p-Histone H3/UBD (day 28). Bar = 50 μm. ** $P < 0.01$ vs. untreated controls (Dunnett's or Steel's test).

to *Actb* levels significantly increased in the ADAQ, TCP, and CBX groups, and transcript levels of *Rbl2* after normalization to *Gapdh* levels significantly decreased in the NFT group compared with untreated controls.

At day 28, transcript levels of *Cdkn1a* after normalization to *Actb* and *Gapdh* levels significantly increased in the TCP group, and significantly decreased in the ADAQ group compared with untreated controls. Transcript levels of *Chek1* after normalization to *Actb* and/or *Gapdh* levels significantly increased in the NFT, TCP, and CBX groups compared with untreated controls. Transcript levels of *Mad2l1* after normalization to *Actb* and/or *Gapdh* levels significantly increased in the ADAQ, TCP, and CBX groups compared with untreated controls. Transcript levels of *Mdm2* and *Tp53* after normalization to *Actb* and/or *Gapdh* levels significantly increased in the ADAQ, TCP, and CBX groups compared with untreated controls. Transcript levels of *Mdm2* after normalization to *Gapdh* levels significantly decreased in the NFT group compared with untreated controls. Transcript levels of *Rbl2* after normalization to *Actb* levels significantly increased in the TCP group, and transcript levels of *Rbl2* after normalization to *Gapdh* levels significantly decreased in the NFT group compared with untreated controls.

DISCUSSION

We have previously reported that 28-day administration of carcinogens facilitating cell proliferation induces an increase in immunoreactive cell populations for cell-cycle-related molecules and apoptosis irrespective of the target organ (Kimura *et al.*, 2015a; Taniai *et al.*, 2012a, 2012b; Yafune *et al.*, 2013a, 2013b). In the present study, the renal carcinogens NFT and TCP increased in the number of Ki-67$^+$ cells and cells immunoreactive for cell-cycle-related molecules 3 days after administration, and renal carcinogen ADAQ induced increases at day 28. The non-carcinogenic renal toxicant CBX also showed similar cellular responses at days 3 and 28. We also previously reported that the non-carcinogenic hepatotoxicant promethazine facilitated cell proliferation and showed a similar pattern of increase in cell populations immunoreactive for cell-cycle proteins to that of the hepatocarcinogenic methyleugenol and thioacetamide in the liver (Kimura *et al.*, 2015a). In addition, the number of TUNEL$^+$ cells increased in NFT and TCP groups transiently at day 7, and only in the CBX group at day 28, indicating that a carcinogen-specific response was not observed with regard to apoptosis. These results suggest that increases in the expression of cell-cycle proteins and apoptosis may not be a carcinogen-specific cellular response, and that it may be difficult to detect carcinogen-specific responses by simple analysis of immunoreactive cell populations and apoptosis using a time-course study of 3, 7 and 28 days of administration.

We have previously reported that 28-day administration of hepatocarcinogens upregulated the spindle checkpoint gene *Mad2l1* (Weaver and Cleveland, 2005), the G_2/M checkpoint gene *Chek1* (Patil *et al.*, 2013), *Cdkn1a* encoding p21 ^{Cip1}, and downregulated *Rbl2*, a gene encoding RB family protein that regulates the progression of G_1/S phase (Cobrinik *et al.*, 1996; Cobrinik, 2005), suggestive of an increase in G_2 and M phase-arrested hepatocyte populations and disruption of G_1/S checkpoint function by hepatocarcinogens (Kimura *et al.*, 2015a). However, in a time course administration study of hepatocarcinogens and hepatocarcinogenic promoters for up to 90 days, expression of *Mad2l1*, *Chek1*, *Cdkn1a*, and *Rbl2* mRNA lacked specificity to carcinogens (Kimura *et al.*, 2015b). In the present study, renal carcinogens also did not induce carcinogen-specific expression changes of these genes in any time points. These results suggest that upregulation of *Mad2l1*, *Chek1*, and *Cdkn1a*, and downregulation of *Rbl2* mRNA may not be responsible for carcinogenesis at early stage of repeated administration of carcinogens.

In the present study, renal carcinogens ADAQ and TCP and non-carcinogenic renal toxicant CBX upregulated transcript levels of *Mdm2* and *Tp53* 3 days after administration, with the exception of *Tp53* expression in the ADAQ group at day 3. p53 is known to regulate multiple genes against acute kidney injury, and MDM2 acts as a regulator of p53 function via ubiquitination and proteasomal degradation or retention of inactive p53 in the cytosol (McNicholas and Griffin, 2012). The MDM2 protein is regulated by multisite phosphorylation, and the phosphorylated site determines the function of MDM2 (Meek and Hupp, 2010). In human hepatocellular carcinoma and lung carcinoma cell lines, it is reported that phosphorylation of MDM2 at Ser 166 is induced by growth factor-mediated signaling, which leads to translocation of MDM2 from the cytoplasm to the nucleus for facilitation of p53 degradation (Malmlöf *et al.*, 2007; Mayo and Donner, 2002). Furthermore, it is reported that human breast cancers showed high expression of MDM2 phosphorylation at Ser 166 in association with cell proliferation activity and a poor prognosis (Schmitz *et al.*, 2006). We previously reported that hepatocarcinogens specifically increased transcript levels of *Mdm2* and/or MDM2$^+$ cells phosphorylated at Ser 166, suggestive of facilitation of degradation of p53 and subsequent disruption of G_1/S checkpoint function by hepatocarcinogen treatment (Kimura *et al.*,

2015a, 2015b). However, in the present study, we did not observe a carcinogen-specific increase in p-MDM2$^+$ cells phosphorylated at Ser 166 by renal carcinogens, while mRNA upregulation of *Mdm2* was found with these carcinogens, as with non-carcinogenic renal toxicant CBX from day 3. These results suggest that upregulation of *Mdm2* may be caused by upregulation of p53 in response to the nephrotoxic effects of both renal carcinogens and non-carcinogenic renal toxicants. The lack of induction of phosphorylation of MDM2 at Ser 166 at the early stages of renal carcinogen administration may be responsible for the lack of cell proliferation facilitation, which is different from the hepatocarcinogens.

It is reported that overexpression of UBD suppresses the kinetochore localization of MAD2, a spindle checkpoint molecule, during the M phase, which may eventually lead to chromosomal instability (Herrmann *et al.*, 2007; Lim *et al.*, 2006). It has also been reported that the UBD-MAD2 interaction reduces the proliferating cell population at M phase, reflecting spindle checkpoint disruption (Theng *et al.*, 2014). We have previously reported that 28- or 90-day administration of carcinogens irrespective of their potential to induce facilitation of cell proliferation causes aberrant expression of UBD at the G_2 phase and a reduction in the ratio of proliferative cells existing at the M phase, indicating disruption of spindle checkpoint function (Kimura *et al.*, 2015a, 2015b; Taniai *et al.*, 2012b). In the present study, the renal carcinogens ADAQ and TCP facilitated cell proliferation and also reduced the ratio of UBD$^+$ cells coexpressing p-Histone H3 to the total number of UBD$^+$ cells and the ratio of p-Histone H3$^+$ cells to that of Ki-67$^+$ cells at day 28. In contrast, the non-carcinogenic renal toxicant CBX only temporarily reduced UBD$^+$ cells coexpressing p-Histone H3 at day 3, but without the accompanied reduction in the ratio of p-Histone H3$^+$ cells to that of Ki-67$^+$ cells. Because p-Histone H3 is an M phase protein (Hirota *et al.*, 2005), these results suggest that renal carcinogens may cause insufficient UBD expression at the M phase, probably in conjunction with the early transition of proliferating cells from the M phase at day 28, in contrast to no such response with non-carcinogenic renal toxicants. Therefore, disruption of spindle checkpoint function may be a key event for carcinogenesis at early stage of repeated administration of carcinogens, and it may take 28 days to induce disruption of spindle checkpoint function by renal carcinogens. On the other hand, TCP also decreased UBD$^+$ cells at M phase at day 7 of administration, while other renal carcinogens did not induce similar cellular responses at this time point. TCP also decreased proliferating cells at M phase at this time point, suggesting that TCP may disrupt spindle checkpoint function at the time point as early as day 7 of administration.

In contrast to ADAQ and TCP, the renal carcinogen NFT did not show a reduction in the number of UBD$^+$ cells coexpressing p-Histone H3 and in the ratio of p-Histone H3$^+$ cells to that of Ki-67$^+$ cells at any time point in the present study, while NFT facilitated cell proliferation activity at all time points. It is reported that a 2-year carcinogenicity study on NFT using rats induced a marginal, but significant, increase in the incidence of renal tubular neoplasms as assessed using additional step-sections of the left and right kidney from each rat; however, the increase was not initially detected after the evaluation using standard single sections (NTP, 1989), suggestive of marginal renal carcinogenic potential of NFT. Both ADAQ and TCP apparently increased the incidence of renal tumors in their 2-year carcinogenicity studies (NTP, 1993a; NTP, 1996). We have reported that leucomalachite green exerting marginal hepatocarcinogenicity did not reduce the ratio of p-Histone H3$^+$ cells to that of Ki-67$^+$ cells by repeated administration for up to 90 days (Kimura *et al.*, 2015b). Therefore, disruption of spindle checkpoint function may not be induced by renal carcinogens exerting marginal carcinogenicity. Cell-cycle facilitation by NFT may be a reflection of the toxic effect of NFT on renal tubules in the present study.

We have previously found that renal carcinogens are associated with development of nephropathy or karyomegaly without relation to genotoxic potentials in a review of the results of carcinogenicity bioassays by the NTP (Taniai *et al.*, 2012a). Among renal carcinogens tested in the present study, repeated administration of ADAQ or TCP to rats has been shown to induce karyomegaly in renal tubular cells (NTP, 1993a; NTP, 1996), while NFT has been shown to induce nephropathy (NTP, 1989). In the present study, NFT, which did not induce karyomegaly, did not cause disruption of spindle checkpoint function. These results may suggest that the ability to induce karyomegaly to carcinogenic target cells is involved in the induction of spindle checkpoint dysfunction. On the other hand, hepatocarcinogen CRB, which did not induce karyomegaly even after 90 days of administration, also caused disruption of spindle checkpoint function (Kimura *et al.*, 2015b). Therefore, disruption of spindle checkpoint function may also be induced by renal carcinogens that do not cause karyomegaly in target tubular cells after repeated administration.

Because carcinogens may exert genotoxicity or trigger oxidative stress responses in relation with carcinogenesis, it is possible that these potentials are involved in disruption of spindle checkpoint function. With regard

to the genotoxic potential of renal carcinogens used in the present study, previous reports suggested that NFT, ADAQ, and TCP are all categorized as genotoxic renal carcinogens (NTP, 1989; NTP, 1993a; NTP, 1996). It is also reported that NFT induced oxidative DNA damage to rat kidney after 28-day repeated oral administration of the carcinogenic dose level (Kijima *et al.*, 2015). However, NFT did not cause disruption of spindle checkpoint function in the present study. These results suggest that it is difficult to find the relationship between the potential to induce spindle checkpoint dysfunction and genotoxic potential of renal carcinogens. Of note, we have shown disruption of spindle checkpoint function in liver cells after repeated 28-day administration of non-genotoxic hepatocarcinogens, i.e., thioacetamide and methapyrilene, in rats (Kimura *et al.*, 2015a, 2015b; Omura *et al.*, 2014). These results suggest that spindle checkpoint dysfunction may be caused by carcinogens without relationship to their genotoxic potential.

In conclusion, both renal carcinogens and non-carcinogenic renal toxicants facilitating cell proliferation increased the number of cells expressing cell-cycle proteins following treatment for up to 28 days, indicating the difficulty in predicting the carcinogenic potential of chemicals by immunohistochemical single molecule analysis in the framework of a 28-day toxicity study. By means of mRNA expression analysis, carcinogen-specific responses in the transcript expression of cell-cycle regulator genes were also lacking following treatment for up to 28 days, which differed from hepatocarcinogens. In contrast, the renal carcinogens ADAQ and TCP reduced the number of cells expressing UBD and the number of proliferating cells at the M phase, suggesting insufficient UBD expression at the M phase and early transition of proliferating cells from M phase, but without the accompanied increase in apoptosis, after 28 days of administration. However, NFT, which has been shown to exert marginal carcinogenic potential, did not induce such cellular responses. These results suggest that it may take 28 days to induce spindle checkpoint dysfunction by renal carcinogens; however, induction of apoptosis may not be essential for this disruption. In contrast, marginal carcinogens may not exert sufficient responses even after 28 days of administration. Further studies may be necessary on the mechanism playing a role for the disruption of spindle checkpoint functions, especially in terms of the molecular interaction of UBD and other regulator molecules after repeated administration of carcinogens.

ACKNOWLEDGMENTS

The authors thank Mrs. Shigeko Suzuki for her technical assistance in preparing the histological specimens. This work was supported by Health and Labour Sciences Research Grants (Research on Food Safety) from the Ministry of Health, Labour and Welfare of Japan (Grant No. H25-shokuhin-ippan-005). M.K. is a Research Fellow of the Japan Society for the Promotion of Science.

Conflict of interest---- The authors declare that there is no conflict of interest.

REFERENCES

Cobrinik, D., Lee, M.H., Hannon, G., Mulligan, G., Bronson, R.T., Dyson, N., Harlow, E., Beach, D., Weinberg, R.A. and Jacks, T. (1996): Shared role of the pRB-related p130 and p107 proteins in limb development. Genes Dev., **10**, 1633-1644.

Cobrinik, D. (2005): Pocket proteins and cell cycle control. Oncogene, **24**, 2796-2809.

Eastin, W.C. (1998): The U.S. National toxicology program evaluation of transgenic mice as predictive models for identifying carcinogens. Environ. Health Perspect., **106**, 81-84.

Herrmann, J., Lerman, L.O. and Lerman, A. (2007): Ubiquitin and ubiquitin-like proteins in protein regulation. Circ. Res., **100**, 1276-1291.

Hirota, T., Lipp, J.J., Toh, B.H. and Peters, J.M. (2005): Histone H3 serine 10 phosphorylation by Aurora B causes HP1 dissociation from heterochromatin. Nature, **438**, 1176-1180.

Jonker, M.J., Bruning, O., van Iterson, M., Schaap, M.M., van der Hoeven, T.V., Vrieling, H., Beems, R.B., de Vries, A., van Steeg, H., Breit, T.M. and Luijten, M. (2009): Finding transcriptomics biomarkers for *in vivo* identification of (non-)genotoxic carcinogens using wild-type and Xpa/p53 mutant mouse models. Carcinogenesis, **30**, 1805-1812.

Kijima, A., Ishii, Y., Takasu, S., Matsushita, K., Kuroda, K., Hibi, D., Suzuki, Y., Nohmi, T. and Umemura, T. (2015): Chemical structure-related mechanisms underlying *in vivo* genotoxicity induced by nitrofurantoin and its constituent moieties in gpt delta rats. Toxicology, **331**, 125-135.

Kimura, M., Abe, H., Mizukami, S., Tanaka, T., Itahashi, M., Onda, N., Yoshida, T. and Shibutani, M. (2015a): Onset of hepatocarcinogen-specific cell proliferation and cell cycle aberration during the early stage of repeated hepatocarcinogen administration in rats. J. Appl. Toxicol., DOI: 10.1002/jat.3163.

Kimura, M., Mizukami, S., Watanabe, Y., Hasegawa-Baba, Y., Onda, N., Yoshida, T. and Shibutani, M. (2015b): Disruption of spindle checkpoint function ahead of facilitation of cell proliferation by repeated administration of hepatocarcinogens in rats. J. Toxicol. Sci., **40**, 855-871.

Lim, C.B., Zhang, D. and Lee, C.G. (2006): FAT10, a gene up-regulated in various cancers, is cell-cycle regulated. Cell Div., **1**, 20.

Livak, K.J. and Schmittgen, T.D. (2001): Analysis of relative gene expression data using real-time quantitative PCR and the $2^{-\Delta\Delta C_T}$ method. Methods, **25**, 402-408.

Malmlöf, M., Roudier, E., Högberg, J. and Stenius, U. (2007): MEK-ERK-mediated phosphorylation of Mdm2 at Ser-166 in

hepatocytes. Mdm2 is activated in response to inhibited Akt signaling. J. Biol. Chem., **282**, 2288-2296.

Matsumoto, H., Saito, F. and Takeyoshi, M. (2014): CARCINOscreen®: New short-term prediction method for hepatocarcinogenicity of chemicals based on hepatic transcript profiling in rats. J. Toxicol. Sci., **39**, 725-734.

Mattila, R., Alanen, K. and Syrjänen, S. (2007): Immunohistochemical study on topoisomerase IIα, Ki-67 and cytokeratin-19 in oral lichen planus lesions. Arch. Dermatol. Res., **298**, 381-388.

Mayo, L.D. and Donner, D.B. (2002): The PTEN, Mdm2, p53 tumor suppressor-oncoprotein network. Trends Biochem. Sci., **27**, 462-467.

McNicholas, B.A. and Griffin, M.D. (2012): Double-edged sword: a p53 regulator mediates both harmful and beneficial effects in experimental acute kidney injury. Kidney Int., **81**, 1161-1164.

Meek, D.W. and Hupp, T.R. (2010): The regulation of MDM2 by multisite phosphorylation—opportunities for molecular-based intervention to target tumours? Semin Cancer Biol., **20**, 19-28.

NTP (1989): NTP Toxicology and Carcinogenesis Studies of Nitrofurantoin (CAS No. 67-20-9) in F344/N Rats and B6C3F1 Mice (Feed Studies). Natl. Toxicol. Program Tech. Rep. Ser., **341**, 1-218.

NTP (1993a): NTP Toxicology and Carcinogenesis of 1,2,3-Trichloropropane (CAS No. 96-18-4) in F344/N Rats and B6C3F1 Mice (Gavage Studies). Natl. Toxicol. Program Tech. Rep. Ser., **384**, 1-348.

NTP (1993b): NTP Toxicology and Carcinogenesis Studies of Triamterene (CAS No. 396-01-0) in F344/N Rats and B6C3F1 Mice (Feed Studies). Natl. Toxicol. Program Tech. Rep. Ser., **420**, 1-367.

NTP (1996): NTP Toxicology and Carcinogenesis Studies of 1-Amino-2,4-Dibromoanthraquinone (CAS No. 81-49-2) in F344/N Rats and B6C3F1 Mice (Feed Studies). Natl. Toxicol. Program Tech. Rep. Ser., **383**, 1-370.

NTP (1998): NTP Toxicology and Carcinogenesis Studies of 1-Chloro-2-propanol (Technical Grade) (CAS NO. 127-00-4) in F344/N Rats and B6C3F1 Mice (Drinking Water Studies). Natl. Toxicol. Program Tech. Rep. Ser., **477**, 1-264.

Omura, K., Uehara, T., Morikawa, Y., Hayashi, H., Mitsumori, K., Minami, K., Kanki, M., Yamada, H., Ono, A. and Urushidani, T. (2014): Detection of initiating potential of non-genotoxic carcinogens in a two-stage hepatocarcinogenesis study in rats. J. Toxicol. Sci., **39**, 785-794.

Patil, M., Pabla, N. and Dong, Z. (2013): Checkpoint kinase 1 in DNA damage response and cell cycle regulation. Cell. Mol. Life Sci., **70**, 4009-4021.

Schmitz, K.J., Grabellus, F., Callies, R., Wohlschlaeger, J., Otterbach, F., Kimmig, R., Levkau, B., Schmid, K.W. and Baba, H.A. (2006): Relationship and prognostic significance of phospho-(serine 166)-murine double minute 2 and Akt activation in node-negative breast cancer with regard to p53 expression. Virchows Arch., **448**, 16-23.

Scholzen, T. and Gerdes, J. (2000): The Ki-67 protein: from the known and the unknown. J. Cell. Physiol., **182**, 311-322.

Tamano, S. (2010): Carcinogenesis risk assessment of chemicals using medium-term carcinogenesis bioassays. Asian Pac. J. Cancer Prev., **11**, 4-5.

Taniai, E., Hayashi, H., Yafune, A., Watanabe, M., Akane, H., Suzuki, K., Mitsumori, K. and Shibutani, M. (2012a): Cellular distribution of cell cycle-related molecules in the renal tubules of rats treated with renal carcinogens for 28 days: relationship between cell cycle aberration and carcinogenesis. Arch. Toxicol., **86**, 1453-1464.

Taniai, E., Yafune, A., Hayashi, H., Itahashi, M., Hara-Kudo, Y., Suzuki, K., Mitsumori, K. and Shibutani, M. (2012b): Aberrant activation of ubiquitin D at G_2 phase and apoptosis by carcinogens that evoke cell proliferation after 28-day administration in rats. J. Toxicol. Sci., **37**, 1093-1111.

Theng, S.S., Wang, W., Mah, W.C., Chan, C., Zhuo, J., Gao, Y., Qin, H., Lim, L., Chong, S.S., Song, J. and Lee, C.G. (2014): Disruption of FAT10-MAD2 binding inhibits tumor progression. Proc. Natl. Acad. Sci. U.S.A., **111**, E5282-5291.

USEPA (2004): Reregistration Eligibility Decision for Carboxin. US. Environmental Protection Agency., Available at: http://www.epa.gov/pesticides/reregistration/REDs/0012red_carboxin.pdf.

Weaver, B.A. and Cleveland, D.W. (2005): Decoding the links between mitosis, cancer, and chemotherapy: The mitotic checkpoint, adaptation, and cell death. Cancer Cell, **8**, 7-12.

Yafune, A., Taniai, E., Morita, R., Nakane, F., Suzuki, K., Mitsumori, K. and Shibutani, M. (2013a): Expression patterns of cell cycle proteins in the livers of rats treated with hepatocarcinogens for 28 days. Arch. Toxicol., **87**, 1141-1153.

Yafune, A., Taniai, E., Morita, R., Hayashi, H., Suzuki, K., Mitsumori, K. and Shibutani, M. (2013b): Aberrant activation of M phase proteins by cell proliferation-evoking carcinogens after 28-day administration in rats. Toxicol. Lett., **219**, 203-210.